ADVANCED MATERIALS
www.advmat.de

Self-Folded Gripper-Like Architectures from Stimuli-Responsive Bilayers

*Arif M. Abdullah, Xiuling Li, Paul V. Braun, John A. Rogers, and K. Jimmy Hsia**

Self-folding microgrippers are an emerging class of smart structures that have widespread applications in medicine and micro/nanomanipulation. To achieve their functionalities, these architectures rely on spatially patterned hinges to transform into 3D configurations in response to an external stimulus. Incorporating hinges into the devices requires the processing of multiple layers which eventually increases the fabrication costs and actuation complexities. The goal of this work is to demonstrate that it is possible to achieve gripper-like configurations in an on-demand manner from simple planar bilayers that do not require hinges for their actuation. Finite element modeling of bilayers is performed to understand the mechanics behind their stimuli-responsive shape transformation behavior. The model predictions are then experimentally validated and axisymmetric gripper-like shapes are realized using millimeter-scale poly(dimethylsiloxane) bilayers that undergo differential swelling in organic solvents. Owing to the nature of the computational scheme which is independent of length scales and material properties, the guidelines reported here would be applicable to a diverse array of gripping systems and functional devices. Thus, this work not only demonstrates a simple route to fabricate functional microgrippers but also contributes to self-assembly in general.

The realization of smart structures capable of autonomous reconfiguration in response to an external stimulus has the potential to revolutionize multiple technological disciplines by allowing humans an unprecedented control over the actuation of functional devices across length and time scales. Consequently, researchers are actively pursuing this line of research and, like many other fields, they have looked into the nature for inspiring design paradigms. In nature, nonmuscular plants respond to changes in their surroundings by generating a variety of movements. Through control mechanisms (both active and passive) plants trigger water transport in and out of their layered cellular architectures, which eventually results in their shape transformation by generating differential turgor.[1,2] The fundamental understandings of plant responsive behavior have been utilized to design multilayer systems where the constituent layers demonstrate different mechanical behaviors in response to externally applied stimuli such as electric fields, residual stress, electrochemical interactions, pH, biochemical enzymes, solvent concentration, moisture content, temperature, and light.[3–14] The above-mentioned structural framework has been used to achieve functionalities in a variety of disciplines including electronics, optics, energy storage, robotics, microfluidics, sensing, actuation, tissue engineering, and drug delivery.[5,7,9,10,15–21]

Within the broad range of stimuli-responsive devices, self-folding grippers are of specific interest due to their biomedical applications. Tetherless, autonomous grippers undergoing shape reconfiguration in response to temperature, residual stress, biochemical entities, and enzymes have been used for biopsy (in vitro and in vivo), drug delivery, and single cell studies.[8,11,22–25] These multilayer gripper designs were motivated by the prehensile biological hands seen in primates. Similar to hands, the grippers had a central section and several finger-like protrusions with spatially separated hinges. Owing to their differences in geometric and/or material characteristics from their surroundings, hinges in self-actuating devices introduce

Dr. A. M. Abdullah
Department of Mechanical Science and Engineering
University of Illinois at Urbana-Champaign
Urbana, IL 61801, USA
Prof. X. Li
Department of Electrical and Computer Engineering
University of Illinois at Urbana-Champaign
Urbana, IL 61801, USA
Prof. P. V. Braun
Department of Materials Science and Engineering
Frederick Seitz Materials Research Laboratory
University of Illinois at Urbana-Champaign
Urbana, IL 61801, USA
Prof. J. A. Rogers
Center for Bio-Integrated Electronics
Departments of Materials Science and Engineering
Biomedical Engineering, Chemistry, Mechanical Engineering
Electrical Engineering and Computer Science, and Neurological Surgery
Simpson Querrey Institute for Nano/Biotechnology
McCormick School of Engineering
Feinberg School of Medicine
Northwestern University
Evanston, IL 60208, USA
Prof. K. J. Hsia
Departments of Mechanical Engineering and Biomedical Engineering
Carnegie Mellon University
Pittsburgh, PA 15213, USA
E-mail: kjhsia@cmu.edu

DOI: 10.1002/adma.201801669

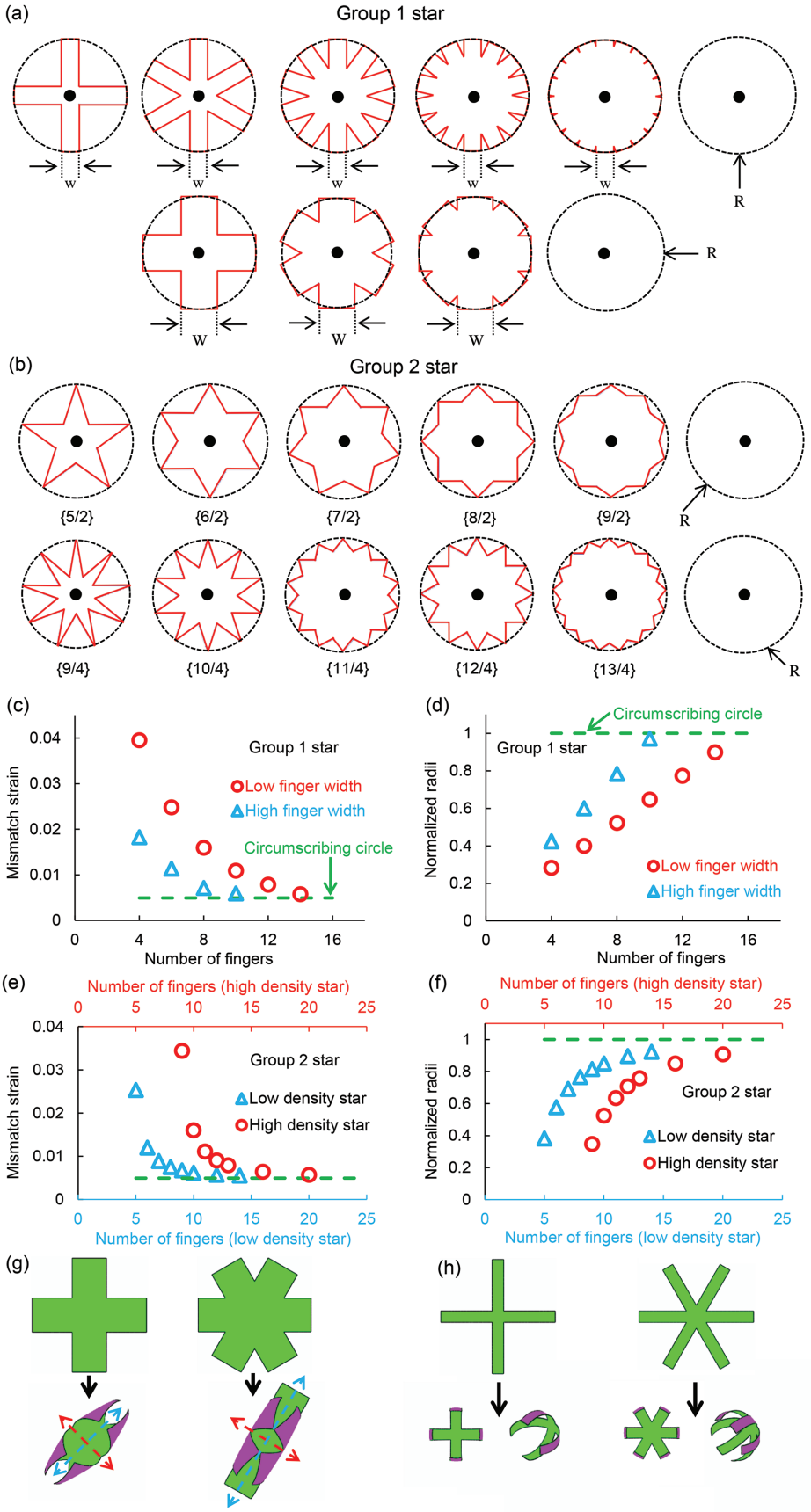

bending stiffness variations and thus make it possible to locally control the curvature of folding in response to external stimuli.[26–28] The hinged microgrippers reported in the literature were fabricated by using conventional processing techniques including photolithography patterning, thin film deposition, and etching. Due to the multilayer nature, these devices require many processing steps and thus become expensive as the cost of microfabricated devices depends on the number of masks needed, design complexities, cleanroom equipment used, required chemical reagents, and processing time.[29] Moreover, having more layers might increase the number of defects within the devices, thereby compromising the robustness of their functionalities. Replacing the hinged multilayer architectures by simple bilayer systems of uniform thickness will not only simplify the current fabrication procedures for the grippers but also elucidate unique design principles for self-folding systems with diverse functionalities.

In stimuli-responsive planar bilayers, the actuation scheme arises from the strain mismatch as one layer expands more than the other one in response to an external stimulus. Although the basic mechanism is straightforward, the shape transformation behavior of bilayer systems depends strongly on their geometric configurations. While beam-like bilayers (width << length) undergo simple uniaxial bending,[30] bilayer plates (width ≈ length) experience both bending and stretching due to isotropic mismatch strains (applied stimulus). At low strains, the bilayers morph into quasi-axisymmetric shapes with nonzero Gaussian curvatures through a combination of out-of-plane bending and in-plane stretching. This combination is energetically expensive at high strains. Hence, the bilayers bifurcate into approximately singly curved states at critical strains.[31–33] Although bifurcation of equilibrium shapes is a universal phenomenon, the occurrence of bifurcation could be tuned through initial bilayer shapes.[34] For gripping functionalities, planar bilayers need to morph into axisymmetric cage-like configurations, where bifurcation into singly curved states needs to be prevented up to high strains. In this paper, through a combination of computation and experiments, we investigated the bifurcation behavior of star-shaped bilayer samples and identified the design principles for generating tetherless gripper-like configurations in an on-demand manner. To gain a mechanistic understanding of bilayer morphing in response to an external stimulus, we employed the finite element method (FEM). We validated the FEM predictions by performing swelling experiments of mm-scale crosslinked poly(dimethylsiloxane) (PDMS) samples in organic solvents. As our computational model is based on the theory of elasticity which is independent of length scales and material properties, the results of our work would be applicable to the diverse array of self-folding systems mentioned earlier.

We start by describing the geometric parameters of the star-shaped bilayers investigated in this work. The protocol for generating star polygons from discrete points has been described in the Supporting Information (Figure S1, Supporting Information). In brief, we considered two star groups with rectangular (Group 1) or triangular (Group 2) finger profiles where the stars approached their circumscribing circles with increasing number of fingers (**Figure 1**a,b). In addition to the circumscribing circle radius R, Group 1 star shapes depend on their finger width (W or w) and Group 2 star shapes depend on their density parameters (low density with Schlafli symbol[35] $\{5/2\}$, $\{6/2\}$, $\{7/2\}$, and so on and high density with Schlafli symbol $\{9/4\}$, $\{10/4\}$, $\{11/4\}$, and so on). In our FEM computations, all geometric parameters of the bilayer star polygons have been normalized by the bilayer thickness (t).

To establish a mechanistic understanding of the stimulus-responsive morphing behavior of the star polygons, we employed the finite element method using ABAQUS.[36] In our model, we analyzed the shape transformation of the polygons by simulating a hypothetical thermal expansion mismatch problem (as temperature increases, active layer expands more than the passive layer). This strategy has been widely used to probe mismatch strain-driven structural behaviors consisting of diverse material systems and stimuli.[31,34,37–41] We incorporated a small imperfection in our model (the mismatch strains along the two in-plane directions varied by 0.01%) for continuous simulation of the morphing behavior before and after bifurcation.[31,34] In our computations, we used four-node general purpose shell elements (Figure S4, Supporting Information) with finite membrane strains. We performed separate mesh refinement studies to identify the optimum mesh size and used the medial axis algorithm to generate elements throughout the structure. As the goal of the present work was to understand the bifurcation of the bilayer star polygons, and eventually develop design principles for gripper-like architectures, we concentrated on the geometric aspects of the problem, and primarily used linear elastic material properties (Young's modulus of 1.8 MPa and a Poisson's ratio of 0.49) in the FEM computations to avoid extensive experimental and computational efforts. To validate some of the experimental observations through our computational framework, we used a second order Ogden material model (Table S1, Supporting Information). We activated the nonlinear geometry option available in ABAQUS to account for the geometric nonlinearities arising from the large deformation of the samples.

The results of the bifurcation behavior of the star-shaped samples are shown in Figure 1c–f. For Group 1 stars, increasing the number of fingers for the same width or increasing the width for the same number of fingers lowers the bifurcation strain. The trend could be understood by considering the sizes of the star mid-sections (radius of the inscribing circle within a star geometry) which scale as $w/2\sin(\pi/n)$, where w is the width of an individual finger and n is the number of fingers. This

Figure 1. (a) shows Group 1 stars (rectangular finger profile) with varying finger numbers (four, six, eight, and so on) and widths (w and W). (b) shows Group 2 stars (triangular finger profile) with varying finger numbers (five, six, seven, and so on) and densities. For both star groups, the circumscribing circles of radii R (black dashed lines) with their centers (black dot) are also shown. The relationship between the bifurcation mismatch strains (finite element calculations) of the stars, their mid-section sizes (inscribing circle radii), and geometric parameters are shown in (c)–(f). (g) and (h) show the original and transformed configurations of four and six-fingered structures with bigger and smaller finger widths. The stimulus-responsive and passive layers are denoted by purple and green, respectively. The major and minor curvature axes are shown by the red and blue arrows.

scaling relationship (Figure 1d) shows that increasing either the width or the number of fingers increases the mid-section sizes. Since bifurcation occurs to minimize the mid-section stretching,[31,34] and the stretching becomes more difficult for bigger mid-sections, star polygons with higher finger width and/or number of fingers tend to bifurcate at lower mismatch strains. As the two sets of the star polygons shown in Figure 1c have the same circumscribing circle, both of them demonstrate the same value of the limiting critical mismatch strain for bifurcation. Group 2 stars (Figure 1e,f) also show similar behavior where star shapes with a higher number of fingers bifurcate at lower strains. In this case, the mid-sections scale as $[R - R\sin(2\pi/n)\tan(\pi/n)]/\cos(\pi/n)$ for the low-density star polygons and $R\cos(\pi/n) - R\sin(\pi/n)\tan(3\pi/n)$ for the high-density star polygons where R is the radius of the circumscribing circle and n is the number of fingers. For the same number of fingers, star polygons with a higher density have smaller mid-sections than their lower density counterparts, and hence they bifurcate at higher critical strains. Beyond bifurcation, all the polygons continue to maintain their singly curved states by bending along their major curvature axes (the directions along which the bending is preferred). Evolution of curvatures in a bilayer star polygon (pre- and postbifurcation), preferred bending modes beyond bifurcation, and geometry effects on curvature-mismatch strain relationships have been discussed in the Supporting Information (Figures S2–S4, Supporting Information).

To realize axisymmetric gripper-like configurations, the star polygons need to reach high strains before bifurcation so that all of their fingers could come toward the mid-section and eventually create an enclosure. Bifurcated singly curved shapes will not be effective grippers as the object of interest held within them might escape through the openings oriented along their minor curvature axes. As the morphing behavior of the polygons strongly depends on their initial shapes, the critical mismatch strains at bifurcation could be tuned through their geometric parameters. We demonstrate this concept through our FEM calculations in Figure 1g,h where four Group 1 stars with various finger numbers and widths are shown with their transformed configurations at a given mismatch strain (Video S1, Supporting Information, shows the shape transformation behavior of six-fingered stars of varying width). The star polygons with bigger finger widths exhibit an approximately singly curved state (Figure 1g) while the ones with smaller finger widths continue to maintain their prebifurcation axisymmetric configurations (Figure 1h). For polygons with larger finger widths, the out-of-plane bending along the minor curvature axes (shown by the blue arrow) is minute and hence the objects held by these bifurcated stars might escape through those openings. This will not be an issue for polygons with smaller finger widths as the bending is similar along all the directions. Thus, our model shows that it is possible to design gripper-like architectures in a rational manner by understanding the mechanics of the star polygons' shape transformation behavior.

We fabricated mm-sized bilayer PDMS samples (**Figure 2**a) with varying crosslinking densities to experimentally investigate their stimulus-responsive shape transformation behavior. Some of the results of our experiments for the two star groups are shown in Figure S5 in the Supporting Information. Consistent with our FEM calculations, both star groups demonstrated similar trends where bifurcation occurred at lower mismatch strains with bigger finger widths and/or higher number of fingers. While the details are described in the Experimental Section, in brief, we used solvent induced swelling of crosslinked PDMS[40] to realize the mismatch strain (arising from the differential swelling of the two layers) that drives shape transformation of the star-shaped samples. Diffusion of solvent into the crosslinked PDMS network is a complex process where the polymeric gel undergoes changes in its shape and volume by establishing a thermodynamic equilibrium between molecular transport and network deformation.[42] The stimulus-responsive behavior of this type of polymeric gel could be captured through nonlinear material models requiring a variety of experimentally determined parameters such as the free swelling stretch of the network, its shear modulus at the dry state, the extent of the crosslinking density, the volume of the solvent molecules and their chemical potentials.[43]

We performed swelling experiments with bilayer PDMS samples (Figure 2b,c), to demonstrate the gripper-like axisymmetric configurations as well as geometry-mismatch strain–curvature relationships of the polygons. At low mismatch strains, the polygons remain mostly planar with little out-of-plane bending deformation. With increasing mismatch strains, the polygons undergo more out-of-plane displacement and hence their bending curvatures increase. All the bifurcated star polygons (Group 1 stars with bigger width and Group 2 stars) demonstrated the trend where the ones with a higher number of fingers were more curved than those with a lower number of fingers at a given mismatch strain. This happens due to early bifurcation and hence bending initiation along the major curvature axes of the polygons with more fingers. As shown in Figure 2b, our experimental results agree with the modeling predictions (Figure 1g,h), i.e., at similar strains, Group 1 stars with bigger finger width transformed into bifurcated singly curved shapes while the ones with smaller finger width maintained their axisymmetric prebifurcated configurations. When the solvent concentration was reduced, our experiments showed that all polygons lowered their bending curvatures (in a reversible manner) through deswelling. Although Group 2 stars studied in our experiments did not morph into gripper-like shapes due to the bifurcation, it is possible to tune their behavior through a rational selection of their geometric parameters. According to our FEM model (Figure 1e,f), increasing the density of this group of stars while keeping the number of fingers low would impede their bifurcation and enable them to maintain their axisymmetric configurations at high mismatch strains. In Video S2 in the Supporting Information, we further complement our computational results as we show the continuous shape transformation of planar bilayers by placing them in a solvent mixture (mismatch strain = 0.11). This video takes around 6 min in real time to reach final states from their initial configurations (Video S2, Supporting Information, is run 16 times faster). The actuation speed (which is limited by diffusion) could be tuned by modifying the bilayer thickness.

In **Figure 3**a,b and Videos S3 and S4 in the Supporting Information, we show the capabilities of deformed star polygons to retain objects within their grasps at varying mismatch strains. We used a soft PDMS block with a ferritic stainless-steel ball embedded within it and chose one Group 1 star with high

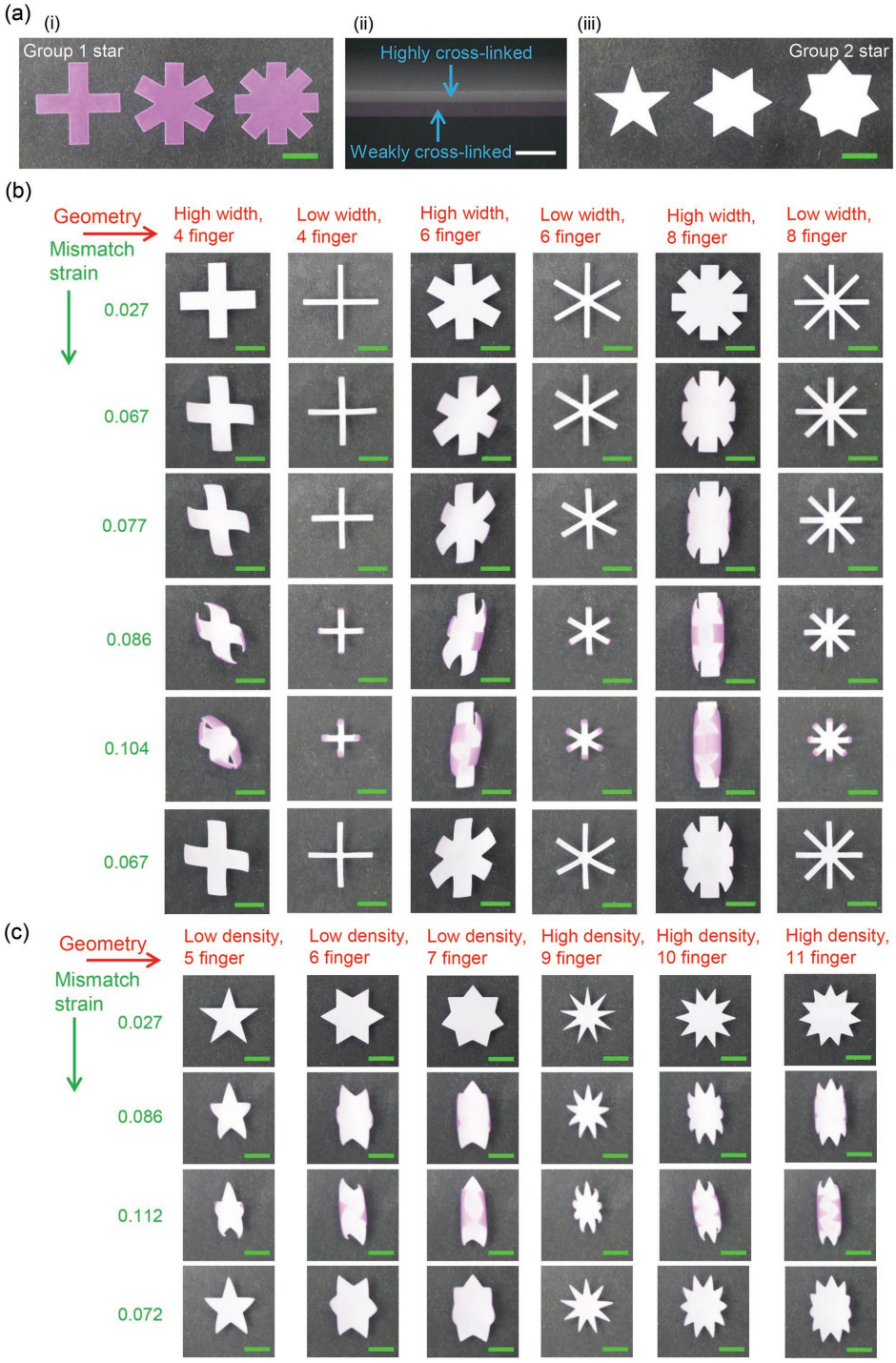

Figure 2. (a) shows the: i,iii) top and ii) cross-sectional views of the fabricated bilayer PDMS samples. (b) and (c) show the evolution of shapes with varying mismatch strains for Group 1 and Group 2 stars. The geometric parameters are: $R/t = 30$, $W/t = 15$ for high finger width, $W/t = 5$ for low finger width, $d = 2$ for low density, and $d = 4$ for high density stars. Scale bars are 5 mm for (a-i,iii), 200 µm for (a-ii), and 5 mm for (b) and (c).

finger width (Video S3, Supporting Information, and Figure 3a) and another one with low finger width (Video S4, Supporting Information, and Figure 3b) for our demonstration. At low mismatch strains, both the star polygons remained mostly flat and the PDMS block moved out of the polygons under the guidance of an external magnetic field applied through a circular magnet outside the container. When the mismatch strain increases, the star polygon with a high finger width bifurcated into a singly curved state and the PDMS block escaped from the star polygon's grasp through the opening along its minor

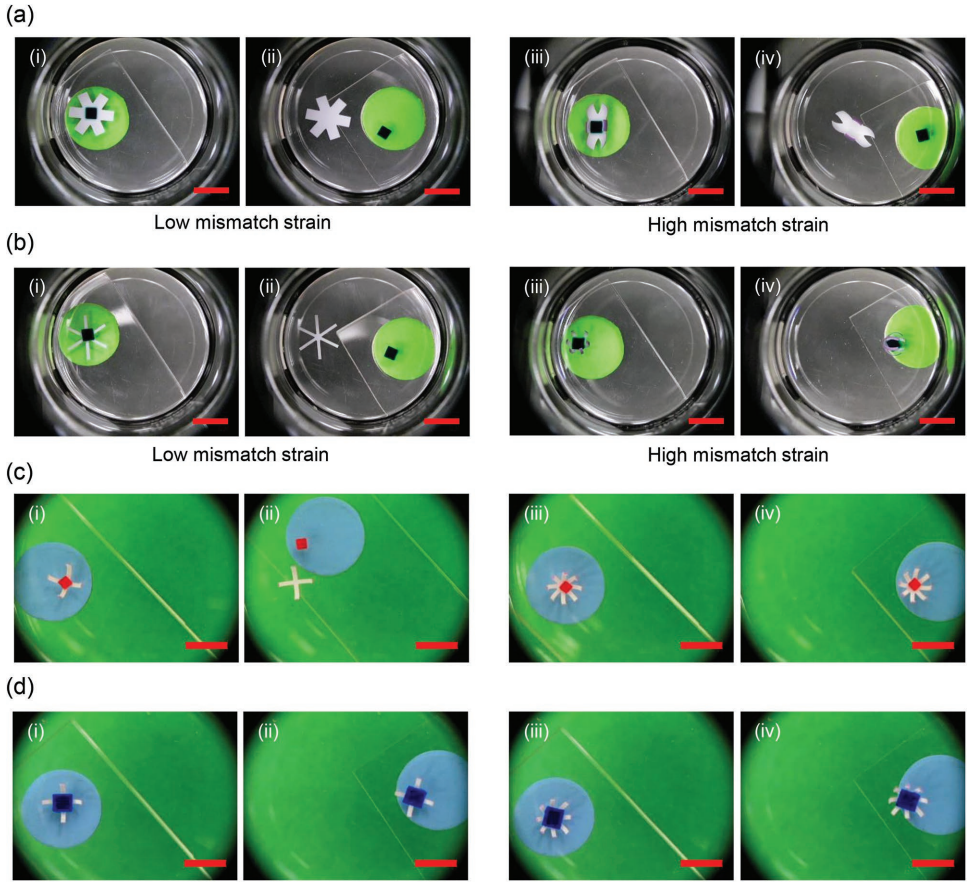

Figure 3. (a) shows a six-fingered star polygon's (bigger finger width) inability to hold onto a PDMS block under an externally applied magnetic field at: i,ii) low and iii,iv) high mismatch strains. (b) shows: i,ii) a six-fingered star polygon's (smaller finger width) inability at low mismatch strains and iii,iv) capability at high mismatch strains to hold onto a PDMS block under an externally applied magnetic field. (c) shows the inability of a four-fingered star and the capability of an eight-fingered star to retain a small PDMS block. (d) shows the capabilities of both the stars to retain a big PDMS block. The geometric parameters are: $R/t = 30$, $W/t = 15$ for (a), and $W/t = 5$ for (b)–(d). All the scale bars are 10 mm.

curvature axis. On the other hand, the star polygon with a low finger width transformed into an axisymmetric shape at high mismatch strains. The PDMS block stayed inside the star polygon and moved with it under magnetic guidance.

We also demonstrated the capabilities of the star polygons to sort objects of different sizes (Figure 3c,d and Videos S5–S8, Supporting Information). We used two magnetically responsive PDMS blocks with 2 mm × 2 mm × 1 mm (red) and 4 mm × 4 mm × 1 mm (blue) dimensions and then experimented with two axisymmetrically deformed (same mismatch strain) Group 1 stars having four and eight fingers. As shown in Videos S5 and S6 in the Supporting Information and Figure 3c, the four-fingered structure failed to hold the smaller red cargo while the eight-fingered star successfully retained the cargo. This selectivity arises from the gap size between the individual fingers. The size-specific selectivity vanishes when the object of interest becomes bigger (Figure 3d and Videos S7 and S8, Supporting Information). These results show the potential of our proposed bilayer structures for size sorting of cargos and capturing biopsy tissue samples of specific sizes for diagnostic purposes. It is worth mentioning that the forces generated at a given finger (within a star) would be directly proportional to its curvature values (at an applied mismatch strain) and constituent material properties, both of which could be adjusted within the proposed design framework of this paper.

The design principles described so far could be used to achieve highly customizable axisymmetric/asymmetric shapes simply through the differential swelling of a bilayer system. We present some examples of this idea in **Figure 4**a where four, six, and five-fingered stars of different geometries are shown at low and high mismatch strains. Through the modification of individual finger widths within a given star geometry, we were able to tune the postbifurcated bending directions and achieve transformed configurations with selectively actuated fingers (e.g., two fingers of a four-fingered star, two and four fingers of a six-fingered star, etc.). Selective actuation of gripper fingers is often desirable for certain gripping and soft robotic applications and on this front, tethered means of actuation (such as electrical, pneumatic, and hydraulic) have been reported in the literature.[10,44–46] Our work complements the existing literature as we show the possibility of achieving tether-less and on-demand selective actuation of self-folding bilayers in response to changes in their environment (chemical stimulus). Tunable pre- and postbifurcated configurations obtained from five-fingered structures establish the applicability of our work to design bilayer stars with an arbitrary number of fingers. We also

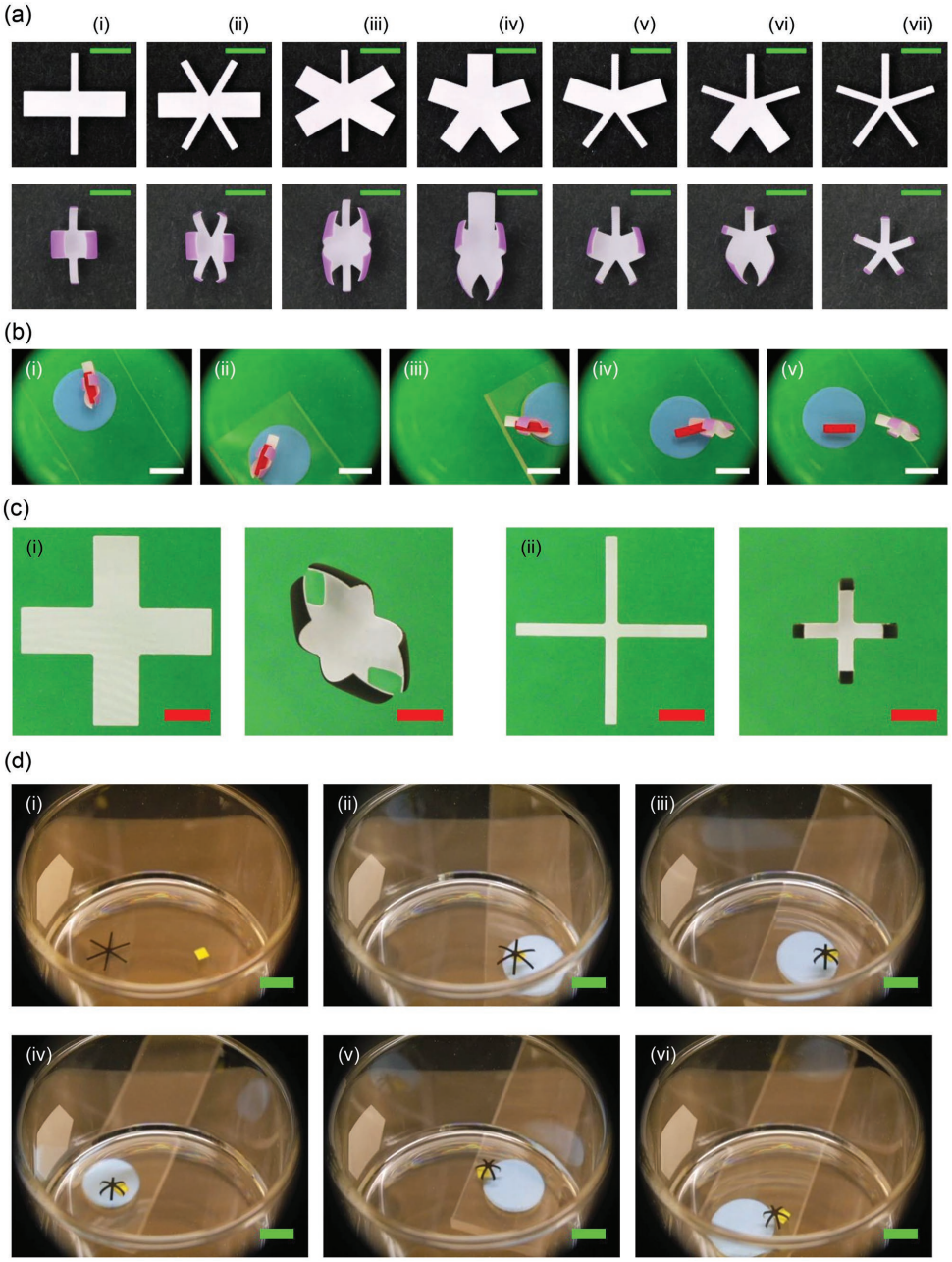

Figure 4. (a) shows the shape transformation behavior of stars with varying geometries. (b) shows the transport and delivery of a PDMS bar by a bifurcated five-fingered star under the guidance of a magnetic field. (c) shows the shape transformation behavior of magnetically responsive four-fingered stars with: i) bigger and ii) smaller finger widths. (d) shows the magnetic guidance of a bilayer star in its planar and curved configurations. It also demonstrates picking-up and placing of an object (yellow-colored) by the bilayered star. The geometric parameters are: $R/t = 30$, $W/t = 15$ for the broader fingers, and $W/t = 5$ for the narrower fingers. Scale bars are 5 mm for (a), 10 mm for (b) and (d), and 3 mm for (c).

experimented with a design reported in the literature[24] where the fingers had rectangular profiles near their mid-sections but became triangular near the tips. Our results show the possibility of achieving asymmetric and axisymmetric shapes at high mismatch strains through the modification of their geometric parameters (Figure S6, Supporting Information).

One possible application of the above-mentioned structures would be to grasp and deliver objects of irregular shapes (e.g., 1D being significantly different from the other two). To demonstrate this idea, we showed in Figure 4b and Video S9 in the Supporting Information that a bifurcated five-fingered structure (Figure 4a-iv), guided by external magnetic field, could "carry" a PDMS block (8 mm × 2 mm × 1 mm) to the desired location and release it. Contrary to the previous demonstrations where the delivery of a "cargo" requires deswelling of the bilayers through changes in the external stimulus, Video S9 in the Supporting Information manifests a different paradigm where the delivery could be

accomplished through the manipulation of the guiding magnetic field.

It should be noted that the formation of gripper-like architectures demonstrated in this work could be achieved through a variety of stimuli-responsive material systems and gripper design schemes. Although we used PDMS to generate gripper-like architectures, our proposed design principles would be applicable to a variety of stimuli-responsive material systems since they are based on our computational framework which is independent of length scales and material properties.[47] In this regard, metals responsive to residual stresses (Cr[23]), oxidative/reductive environments (Cu[48]), and heat (low melting point alloy[49]); polymeric systems responsive to chemical/water diffusion (photoresist[9,23,50] and poly(3,4-ethylenedioxythiophene):polystyrene sulfonate (PEDOT:PSS)[10]), heat (photoresist,[11,23] liquid-crystal elastomer (LCE),[51] and shape-memory polymer (SMP)[52]), light (photoresist,[53] LCE, and SMP[54]), biochemical enzymes (gelatin and carboxymethylcellulose[8]), and magnetic fields (polypyrrole embedded with Ni/Au[55]); hydrogels responsive to heat (pNIPAM[24,56]), water/solvent diffusion (poly(ethylene glycol) diacrylate[57] and poly(glycidyl methacrylate)[58]), salt concentration (poly(methacryloxyethyltrimethylammonium chloride) (PMETAC)[58]), pH (acrylic acid (AA) and 2-(dimethylamino) ethyl methacrylate (DMAEMA)[59]), and light (graphene oxide/polypetide composite[60]); and oxides responsive to residual stresses (SiO/SiO_2[22]) could be incorporated into bilayer architectures to realize stimuli-responsive functional grippers.

Through appropriate chemistry-based and engineering design principles, the above-mentioned material systems could be made responsive to multiple stimuli without sacrificing their performance/structural integrity. We manifest this concept by fabricating bilayer PDMS samples that are responsive to both solvent concentrations and external magnetic fields. As shown in Figure 4c,d and Video S10 in the Supporting Information the bilayer sample demonstrated asymmetric/axisymmetric deformation behavior at high mismatch strains and followed the magnetic guidance at both planar and curved configurations. Video S10 in the Supporting Information also shows the capabilities of the bilayered structures to be directed to a desired cargo, enclose it through axisymmetric folding, and deliver it to a distant location. These illustrations build upon the design principles proposed through our research and present opportunities for autonomous multifield responsive picking/placing, cargo delivery, and soft robotic functionalities without on-board power sources and control systems.

In conclusion, our work establishes the design principles to realize gripper-like configurations from stimuli-induced folded bilayers in a tetherless and on-demand manner. We developed finite element models of the stimuli-responsive shape transformation behavior of the bilayers. The computational predictions have been verified experimentally with millimeter-scale PDMS bilayer samples upon differential swelling in organic solvents. As examples, we demonstrated the capabilities of these architectures to retain, transport, and deliver cargos of different sizes in an as-required manner. We also achieved varying degrees of selective actuation of the bilayered stars in response to a uniformly applied stimulus. As the finite element technique is independent of length scales and material properties, the proposed design principles would be applicable to a diverse array of gripping/soft robotic systems consisting of different geometric parameters and/or material systems responsive to single/multiple stimuli (also demonstrated in this work). Besides proposing a simple route to fabricate microgrippers, our work contributes to self-assembly in general and hence, the findings could be used to realize a wide variety of stimuli-responsive functional devices.

Experimental Section

See the Supporting Information for details of the experimental protocol.

Supporting Information

Supporting Information is available from the Wiley Online Library or from the author.

Acknowledgements

A.M.A. acknowledges support from the Food Machinery Corporation (FMC) Educational Fund Fellowship and the Graduate College Dissertation Completion Fellowship through the University of Illinois at Urbana-Champaign. The authors acknowledge partial support from the U.S. Department of Energy, Office of Science, Basic Energy Sciences, under Award No. DE-FG02-07ER46471. K.J.H. acknowledges partial support from Carnegie Mellon University.

Conflict of Interest

The authors declare no conflict of interest.

Keywords

bifurcation, functional grippers, self-folding, soft robotics, stimuli-responsive

Received: March 14, 2018
Revised: April 20, 2018
Published online: June 19, 2018

[1] J. M. Skotheim, *Science* **2005**, *308*, 1308.
[2] Y. Forterre, *J. Exp. Bot.* **2013**, *64*, 4745.
[3] J. S. Randhawa, K. E. Laflin, N. Seelam, D. H. Gracias, *Adv. Funct. Mater.* **2011**, *21*, 2395.
[4] L. Hines, K. Petersen, G. Z. Lum, M. Sitti, *Adv. Mater.* **2017**, *29*, 1603483.
[5] W. Huang, X. Yu, P. Froeter, R. Xu, P. Ferreira, X. Li, *Nano Lett.* **2012**, *12*, 6283.
[6] E. W. H. Jager, *Science* **2000**, *288*, 2335.
[7] H. He, J. Guan, J. L. Lee, *J. Controlled Release* **2006**, *110*, 339.
[8] N. Bassik, A. Brafman, A. M. Zarafshar, M. Jamal, D. Luvsanjav, F. M. Selaru, D. H. Gracias, *J. Am. Chem. Soc.* **2010**, *132*, 16314.
[9] M. Jamal, A. M. Zarafshar, D. H. Gracias, *Nat. Commun.* **2011**, *2*, 527.
[10] S. Taccola, F. Greco, E. Sinibaldi, A. Mondini, B. Mazzolai, V. Mattoli, *Adv. Mater.* **2015**, *27*, 1668.

[11] E. Gultepe, J. S. Randhawa, S. Kadam, S. Yamanaka, F. M. Selaru, E. J. Shin, A. N. Kalloo, D. H. Gracias, *Adv. Mater.* **2013**, *25*, 514.
[12] A. A. Bauhofer, S. Krödel, J. Rys, O. R. Bilal, A. Constantinescu, C. Daraio, *Adv. Mater.* **2017**, *29*, 1703024.
[13] P. Froeter, X. Yu, W. Huang, F. Du, M. Li, I. Chun, S. H. Kim, K. J. Hsia, J. A. Rogers, X. Li, *Nanotechnology* **2013**, *24*, 475301.
[14] I. S. Chun, A. Challa, B. Derickson, K. J. Hsia, X. Li, *Nano Lett.* **2010**, *10*, 3927.
[15] V. B. Shenoy, D. H. Gracias, *MRS Bull.* **2012**, *37*, 847.
[16] V. A. Bolaños Quiñones, L. Ma, S. Li, M. Jorgensen, S. Kiravittaya, O. G. Schmidt, *Opt. Lett.* **2012**, *37*, 4284.
[17] C. C. Bof Bufon, J. D. Cojal González, D. J. Thurmer, D. Grimm, M. Bauer, O. G. Schmidt, *Nano Lett.* **2010**, *10*, 2506.
[18] W. Xi, A. A. Solovev, A. N. Ananth, D. H. Gracias, S. Sanchez, O. G. Schmidt, *Nanoscale* **2013**, *5*, 1294.
[19] E. J. Smith, S. Schulze, S. Kiravittaya, Y. Mei, S. Sanchez, O. G. Schmidt, *Nano Lett.* **2011**, *11*, 4037.
[20] B. Yuan, Y. Jin, Y. Sun, D. Wang, J. Sun, Z. Wang, W. Zhang, X. Jiang, *Adv. Mater.* **2012**, *24*, 890.
[21] X. Yu, W. Huang, M. Li, T. M. Comberiate, S. Gong, J. E. Schutt-Aine, X. Li, *Sci. Rep.* **2015**, *5*, 9661.
[22] K. Malachowski, M. Jamal, Q. Jin, B. Polat, C. J. Morris, D. H. Gracias, *Nano Lett.* **2014**, *14*, 4164.
[23] T. G. Leong, C. L. Randall, B. R. Benson, N. Bassik, G. M. Stern, D. H. Gracias, *Proc. Natl. Acad. Sci. USA* **2009**, *106*, 703.
[24] J. C. Breger, C. Yoon, R. Xiao, H. R. Kwag, M. O. Wang, J. P. Fisher, T. D. Nguyen, D. H. Gracias, *ACS Appl. Mater. Interfaces* **2015**, *7*, 3398.
[25] K. Malachowski, J. Breger, H. R. Kwag, M. O. Wang, J. P. Fisher, F. M. Selaru, D. H. Gracias, *Angew. Chem., Int. Ed.* **2014**, *53*, 8045.
[26] E. Smela, O. Inganas, I. Lundstrom, *Science* **1995**, *268*, 1735.
[27] E. W. H. Jager, *Science* **2000**, *290*, 1540.
[28] G. P. Nikishkov, *J. Appl. Phys.* **2003**, *94*, 5333.
[29] M. J. Madou, *Fundamentals of Microfabrication and Nanotechnology*, CRC Press, Boca Raton, FL, USA **2012**.
[30] S. Timoshenko, *J. Opt. Soc. Am.* **1925**, *11*, 233.
[31] L. B. Freund, *J. Mech. Phys. Solids* **2000**, *48*, 1159.
[32] N. J. Salamon, C. B. Masters, *Int. J. Solids Struct.* **1995**, *32*, 473.
[33] L. B. Freund, S. Suresh, *Thin Film Materials: Stress, Defect Formation, and Surface Evolution*, Cambridge University Press, New York **2009**.
[34] A. M. Abdullah, P. V. Braun, K. J. Hsia, *Appl. Phys. Lett.* **2017**, *111*, 104101.
[35] H. S. M. Coxeter, *Introduction to Geometry*, Wiley, New York **1989**.
[36] D. Hibbitt, B. Karlsson, P. Sorensen, *ABAQUS*, Dassault Systemes, Providence, RI, USA **2014**.
[37] H. Yang, F. Fan, W. Liang, X. Guo, T. Zhu, S. Zhang, *J. Mech. Phys. Solids* **2014**, *70*, 349.
[38] G. Stoychev, S. Turcaud, J. W. C. Dunlop, L. Ionov, *Adv. Funct. Mater.* **2013**, *23*, 2295.
[39] A. M. Abdullah, K. Nan, J. A. Rogers, K. J. Hsia, *Extreme Mech. Lett.* **2016**, *7*, 34.
[40] A. M. Abdullah, P. V. Braun, K. J. Hsia, *Soft Matter* **2016**, *12*, 6184.
[41] M. J. Motala, D. Perlitz, C. M. Daly, P. Yuan, R. G. Nuzzo, K. J. Hsia, *Extreme Mech. Lett.* **2015**, *3*, 8.
[42] W. Hong, X. Zhao, J. Zhou, Z. Suo, *J. Mech. Phys. Solids* **2008**, *56*, 1779.
[43] W. Hong, Z. Liu, Z. Suo, *Int. J. Solids Struct.* **2009**, *46*, 3282.
[44] S. Bauer, S. Bauer-Gogonea, I. Graz, M. Kaltenbrunner, C. Keplinger, R. Schwödiauer, *Adv. Mater.* **2014**, *26*, 149.
[45] B. Mosadegh, P. Polygerinos, C. Keplinger, S. Wennstedt, R. F. Shepherd, U. Gupta, J. Shim, K. Bertoldi, C. J. Walsh, G. M. Whitesides, *Adv. Funct. Mater.* **2014**, *24*, 2163.
[46] H. Yuk, S. Lin, C. Ma, M. Takaffoli, N. X. Fang, X. Zhao, *Nat. Commun.* **2017**, *8*, 14230.
[47] A. F. Bower, *Applied Mechanics of Solids*, CRC Press, Boca Raton, FL **2010**.
[48] J. S. Randhawa, M. D. Keung, P. Tyagi, D. H. Gracias, *Adv. Mater.* **2010**, *22*, 407.
[49] B. E. Schubert, D. Floreano, *RSC Adv.* **2013**, *3*, 24671.
[50] J. S. Randhawa, T. G. Leong, N. Bassik, B. R. Benson, M. T. Jochmans, D. H. Gracias, *J. Am. Chem. Soc.* **2008**, *130*, 17238.
[51] T. H. Ware, M. E. McConney, J. J. Wie, V. P. Tondiglia, T. J. White, *Science* **2015**, *347*, 982.
[52] W. Voit, T. Ware, R. R. Dasari, P. Smith, L. Danz, D. Simon, S. Barlow, S. R. Marder, K. Gall, *Adv. Funct. Mater.* **2010**, *20*, 162.
[53] K. E. Laflin, C. J. Morris, T. Muqeem, D. H. Gracias, *Appl. Phys. Lett.* **2012**, *101*, 131901.
[54] Y. Yu, T. Ikeda, *Macromol. Chem. Phys.* **2005**, *206*, 1705.
[55] B. Jang, E. Gutman, N. Stucki, B. F. Seitz, P. D. Wendel-García, T. Newton, J. Pokki, O. Ergeneman, S. Pané, Y. Or, B. J. Nelson, *Nano Lett.* **2015**, *15*, 4829.
[56] G. Stoychev, N. Puretskiy, L. Ionov, *Soft Matter* **2011**, *7*, 3277.
[57] H. R. Kwag, J. V. Serbo, P. Korangath, S. Sukumar, L. H. Romer, D. H. Gracias, *Tissue Eng., Part C* **2016**, *22*, 398.
[58] T. S. Kelby, M. Wang, W. T. S. Huck, *Adv. Funct. Mater.* **2011**, *21*, 652.
[59] L. Dong, A. K. Agarwal, D. J. Beebe, H. Jiang, *Nature* **2006**, *442*, 551.
[60] E. Wang, M. S. Desai, S.-W. Lee, *Nano Lett.* **2013**, *13*, 2826.